

Identification of a Suitable Peptidic Molecular Platform for the Development of NPY(Y₁)R-Specific Imaging Agents

Korbinian Krieger,^[a] Björn Wängler,^[b] Ralf Schirmacher,^[c] and Carmen Wängler*^[a]

NPY(Y₁)R (neuropeptide Y receptor subtype 1) is an important target structure for tumor-specific imaging and therapy as this receptor subtype is overexpressed in very high density and incidence especially in human breast cancer. Targeting this receptor with radiolabeled truncated analogues of the endogenous ligand NPY (neuropeptide Y) has, however, not yet resulted in satisfactory imaging results when using positron emission tomography (PET). This can be attributed to the limited stability of these PET imaging agents caused by their fast proteolytic degradation. Although highly promising NPY analogues were developed, their stability has only been investigated in very few cases. In this systematical work, we

comparatively determined the stability of the five most promising truncated analogues of NPY that were developed over the last years, showing the highest receptor affinities and subtype selectivities. The stability of the peptides was assessed in human serum as well as in a human liver microsomal stability assay; these gave complementary results, thus demonstrating the necessity to perform both assays and not just conventional serum stability testing. Of the tested peptides, only [Lys(lauroyl)²⁷,Pro³⁰,Lys(DOTA)³¹,Bip³²,Leu³⁴]NPY₂₇₋₃₆ showed high stability against peptidase degradation; thus this is the best-suited truncated NPY analogue for the development of NPY(Y₁)R-specific imaging agents.

Introduction

Neuropeptide Y (NPY) is a peptide hormone consisting of 36 amino acids and has several regulatory functions in human physiological as well as pathological conditions. It binds to four different G protein-coupled receptors in humans (NPY(Y₁)R, NPY(Y₂)R, NPY(Y₄)R and NPY(Y₅)R) and regulates appetite, hormone secretion, cardiovascular and immune system, bone homeostasis, stress response and anxiety.^[1,2] Furthermore, it is also involved in pathological processes such as obesity, hypertension, atherosclerosis, stress and several mood disorders.^[1]

Recently, it was also found to be associated with different malignancies such as breast, renal cell and ovarian carcinomas, neuro- and neuroblastomas and others.^[3] Especially in breast cancer, NPY(Y₁)R is a highly promising target structure for

tumor-specific imaging and therapy as this receptor subtype is overexpressed in very high density and incidence^[4,5] (85% in primary human breast carcinomas and 100% of lymph node metastases of receptor-positive primaries), whereas non-neoplastic breast tissue only expresses NPY(Y₂)R.

Thus, many attempts were made within the last years to develop radiolabeled NPY(Y₁)R-specific analogues of NPY for the sensitive and specific imaging of this malignancy.^[1] For this purpose, the full-length peptide can in principle be used, but short peptide sequences are much easier to synthesize than long ones and usually show better radiolabeling results as well as improved *in vivo* pharmacokinetics.^[6] Furthermore, the full-length peptide is a pan-receptor ligand, showing no receptor subtype selectivity. Hence, the vast majority of approaches aimed at the development of truncated versions of NPY, ideally showing a strong receptor subtype preference as well as a high affinity to the NPY(Y₁)R. One challenge is that the peptide-receptor interaction was demonstrated to be highly sensitive to structural changes of the peptide. The C-terminal part of the peptide, NPY₂₈₋₃₆, is the minimal core sequence for receptor binding and Arg33, Arg35 as well as the terminal Tyr36-amide are essential for NPY(Y₁)R binding.^[2,7,8] Furthermore, Thr32 and Gln34 were found to be crucial for receptor subtype preference.^[2] These prerequisites limit the possibilities of peptide modification to obtain truncated NPY analogues exhibiting the mentioned properties and being applicable for tumor imaging.

Another, even greater challenge in NPY-based radiotracer development is the physiological degradation of the lead peptide NPY as well as its truncated analogues. This limited stability of physiological peptides is a common phenomenon under *in vivo* conditions and is mainly mediated by proteolytic enzymes occurring in blood, liver and kidney.^[9,10] In case of NPY and its analogues, the degradation is mediated by a vast

[a] K. Krieger, Prof. Dr. C. Wängler
Biomedical Chemistry
Department of Clinical Radiology and Nuclear Medicine
Medical Faculty Mannheim of Heidelberg University
Theodor-Kutzer-Ufer 1–3
68167 Mannheim (Germany)
E-mail: Carmen.Waengler@medma.uni-heidelberg.de

[b] Prof. Dr. B. Wängler
Molecular Imaging and Radiochemistry
Department of Clinical Radiology and Nuclear Medicine
Medical Faculty Mannheim of Heidelberg University
Theodor-Kutzer-Ufer 1–3
68167 Mannheim (Germany)

[c] Prof. Dr. R. Schirmacher
Division of Oncological Imaging, Department of Oncology
University of Alberta
11560 University Avenue
Edmonton, AB T6G 1Z2 (Canada)

© 2020 The Authors. Published by Wiley-VCH GmbH.
This is an open access article under the terms of the Creative Commons Attribution Non-Commercial NoDerivs License, which permits use and distribution in any medium, provided the original work is properly cited, the use is non-commercial and no modifications or adaptations are made.

number of peptidases,^[11] cleaving the peptide at the pharmacophoric Arg33 and Arg35 residues^[12,13] and many other positions of the peptide sequence.^[11] This intrinsically and considerably limits the stability of radiolabeled NPY analogues and thus impedes successful tumor imaging using this peptide family. Of the many developed NPY derivatives, only few were tested for stability and applicability for tumor imaging and when determined, the truncated peptides showed an overall low^[14,15] or significantly decreased stability compared to NPY.^[12] This low stability was attributed to the reduced number of amino acids resulting in a poorly defined secondary structure of these short peptides entailing a faster proteolytic degradation.^[16]

Nevertheless, many truncated NPY analogues – several of them exhibiting very good to excellent *in vitro* properties such as high NPY(Y₁)R affinity and receptor subtype selectivity^[12,14,15,17,18,19,20,21] – were developed with the aim of finding a peptide sequence applicable as NPY(Y₁)R-specific tumor-targeting agent, for instance for molecular imaging. However, respective radiolabeled analogues applied for *in vivo* tumor visualization using highly sensitive *in vivo* PET imaging were seldomly reported and showed suboptimal pharmacokinetics^[15,22] caused by the stability issues discussed above.

One possibility to stabilize radiolabeled peptides against metabolic degradation is to modify them chemically, thereby hampering enzymatic breakdown.^[23] An alternative to this sometimes laborious structural modification in order to achieve higher *in vivo* stabilities of radiopeptides was proposed recently and showed favorable imaging results and strongly increased tumor uptakes. This was coinjection of the radioligands with enzyme inhibitors, protecting the applied GRPR-, SSTR- and CCK2R-specific radiotracers against proteolytic degradation (GRPR: gastrin-releasing peptide receptor, SSTR: somatostatin receptor, CCK2R: cholecystokinin receptor subtype 2).^[24] Although this approach showed in part extremely valuable results, it has to be adapted to the respective peptidic radiotracer to be able to increase its metabolic stability, thus also entailing further optimization steps.^[25,26]

Unfortunately, no stability data are available for most of the developed NPY(Y₁)R-specific ligands and no systematic study has been performed so far directly comparing their metabolic stabilities. As a high stability of the receptor ligands is however a prerequisite for *in vivo* target accumulation and thus tumor visualization, NPY analogues exhibiting the mandatory high stability have to be identified to become lead structures for labeled imaging probes for molecular NPY(Y₁)R imaging.

Thus, we synthesized and directly compared ⁶⁸Ga-radio-labeled analogues of the most promising described truncated NPY analogues^[12,15,17,18,19,20] with regard to their metabolic stability. This comparison was based on *in vitro* stability determinations in human serum as well as human liver microsomal stability assays, both providing a good, quantifiable measure on the intrinsic proteolytic degradation of the peptidic ligands. Although it was shown before that *in vitro* stability studies in serum and organ homogenates cannot predict the *in vivo* metabolism pathway or *in vivo* half-life of the agents, it enables the reliable comparison of relative stabilities and the

identification of compounds with considerably improved metabolic stability.^[27,28] By this, we intended to determine the most promising peptidic lead structure for the development of labeled NPY-derived imaging agents for the visualization of NPY (Y₁)R-expressing tumors.

Results and Discussion

Truncated NPY derivatives chosen for comparative stability assessment

Over the last two decades, nearly 80 truncated peptide analogues of NPY were developed, exhibiting a linear, cyclic or dimeric peptide backbone in order to identify derivatives with high NPY(Y₁)R targeting ability.^[12,14,15,17,18,19,20,21,29,30] Among these, several showed low affinities, NPY(Y₁) receptor subtype selectivities or stabilities. Of those remaining, we chose to directly compare five different peptide analogues regarding their metabolic stability (Figure 1), representing the most promising agents in terms of *in vitro* properties (NPY(Y₁)R affinity, Table 1, and receptor subtype selectivity) within their respective group of linear, cyclic and dimeric truncated NPY analogues: i) linear [Pro³⁰,Lys(DOTA)³¹,Tyr³²,Leu³⁴]NPY₂₈₋₃₆ ([Lys⁴(DOTA)]-BVD₁₅, **1**; DOTA = (1,4,7,10-tetraazacyclododecane-1,4,7,10-tetra-yl)tetraacetic acid), serving as reference compound with known low metabolic stability but high NPY(Y₁)R affinity and receptor subtype selectivity,^[18] ii) [Pro³⁰,Lys(DOTA)³¹,Bip³²,Leu³⁴]NPY₂₈₋₃₆ (**2**), a variant of **1** comprising an artificial Bip (biphenylalanine) amino acid in position 32 instead of tyrosine,^[12] and Lys(DOTA) in position 31 for radiolabeling,^[15] iii) [Lys(lauroyl)]²⁷,Pro³⁰,Lys(DOTA)³¹,Bip³²,Leu³⁴]NPY₂₇₋₃₆ (**3**), a variant of **2** modified with an additional N_ε-Lys-lauroyl in position 27 for full receptor agonism and high NPY(Y₁)R affinity,^[19] also modified with Lys(DOTA) in position 31 for radiolabeling, iv) Ac[D-Cys²⁹,Lys(DOTA)³¹,Cys³⁴]NPY₂₉₋₃₆ (YM-42454, **4**), a cyclic truncated NPY₂₈₋₃₆ analogue developed for conformational fixation, resulting in high NPY(Y₁)R affinity and receptor subtype selectivity^[20] which was also modified with Lys(DOTA)³¹ for radiolabeling, and v) heterodimer [Pro³⁰,Cys³¹,Trp³²,Nle³⁴]NPY₂₈₋₃₆-[Lys(DOTA)²⁹,Pro³⁰,Cys³¹,Trp³²,Nle³⁴]NPY₂₈₋₃₆ (**5**), also displaying a high NPY(Y₁)R affinity.^[17]

For DOTA introduction in analogues **3** and **4**, being required for radiolabeling and comparative stability assessment, we did not modify the respective peptides N-terminally as the N terminus was shown to be important for receptor activation.^[12,18] Alternatively, the chelator can, for example, be conjugated to a side-chain functionality of an additionally introduced amino acid at the N terminus.^[19] However, as it was shown for BVD₁₅ that the DOTA conjugation least impedes peptide-receptor interaction when introduced in position 31 by using Lys(N_ε-DOTA),^[18] we applied this molecular design, resulting in peptide precursors **2**, **3** and **4**. Derivatives **1** and **5** were already described as DOTA-modified agents.

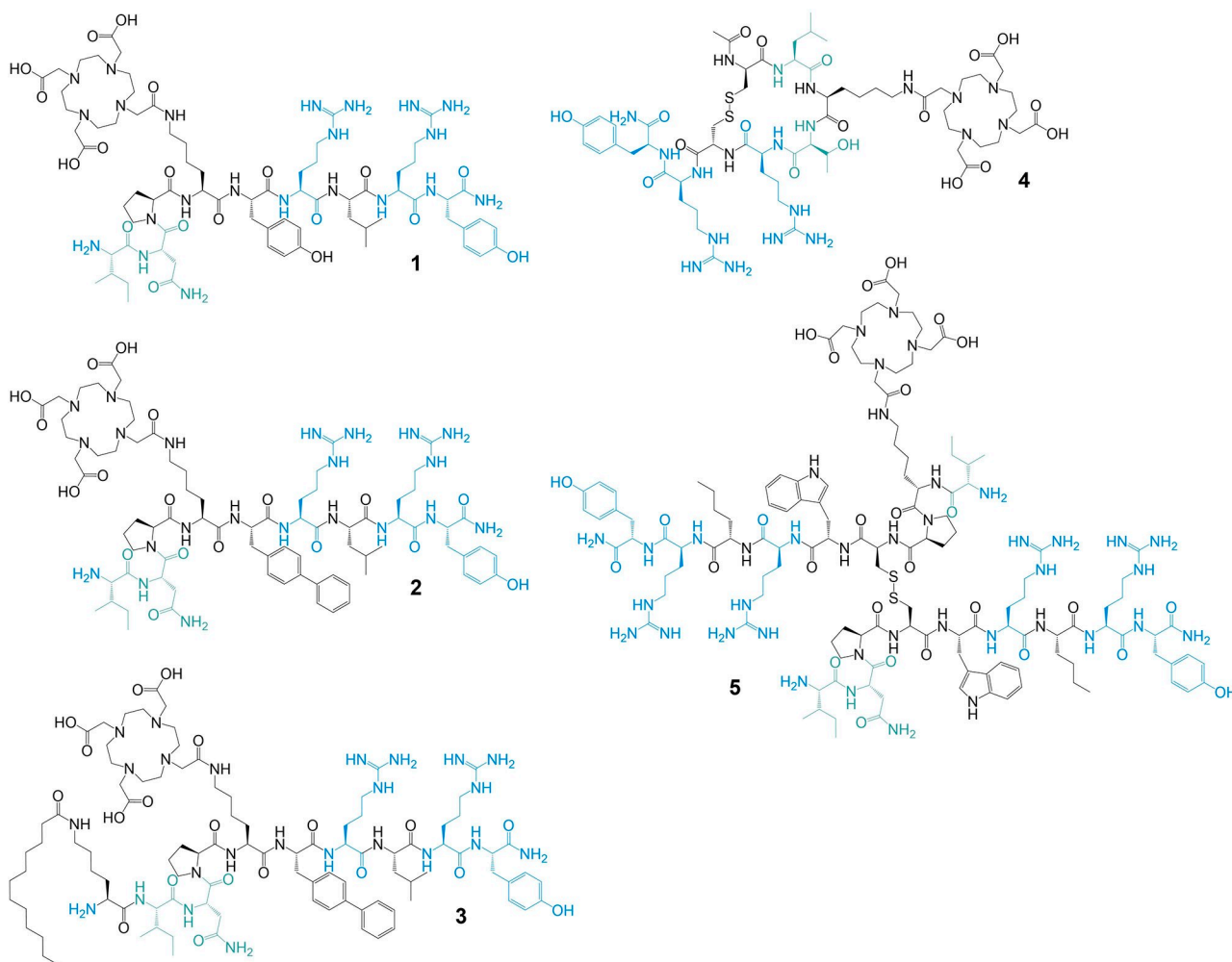


Figure 1. Structures of the investigated truncated and DOTA-modified NPY analogues 1–5. NPY-derived structure elements are highlighted in turquoise, pharmacophoric structure elements for NPY(Y₁)R binding are depicted in sky blue.

Compound	RCY ^[a]	A _m ^[b] [GBq/μmol]	log _D	t _{1/2} ^[c] [min]	t _{1/2} ^[d] [min]	NPY(Y ₁)R affinity [nM]
1/[⁶⁸ Ga]1 HR-ESI-MS (<i>m/z</i>) for [M + 4H] ⁴⁺ (calcd): 402.7305 (402.7314), [M + 3H] ³⁺ (calcd): 536.6383 (536.6393), [M + 2H] ²⁺ (calcd): 804.4537 (804.4550); MALDI-MS (<i>m/z</i>) for [M + H] ⁺ (calcd): 1607.40 (1607.90), [M + Na] ⁺ : 1629.51 (1629.88), [M + K] ⁺ : 1645.50 (1645.86)	99.4%	21.2–23.1	−3.61 ± 0.37	20	> 100	K _i : 7 ± 3 ^{[e][18]}
2/[⁶⁸ Ga]2 HR-ESI-MS (<i>m/z</i>) for [M + 4H] ⁴⁺ (calcd): 417.7397 (417.7405), [M + 3H] ³⁺ : 556.6504 (556.6514); MALDI-MS (<i>m/z</i>) for [M + H] ⁺ (calcd): 1667.83 (1667.94), [M + Na] ⁺ : 1689.90 (1689.92), [M + K] ⁺ : 1705.29 (1705.89)	99.2%	19.0–21.4	−3.01 ± 0.13	65	> 100	IC ₅₀ : 29.7 ± 6.8 ^{[f][12]}
3/[⁶⁸ Ga]3 HR-ESI-MS (<i>m/z</i>) for [M + 4H] ⁴⁺ (calcd): 495.2564 (495.3060), [M + 3H] ³⁺ : 660.0712 (660.0721); MALDI-MS (<i>m/z</i>) for [M + H] ⁺ (calcd): 1978.01 (1978.20), [M + Na] ⁺ : 1999.95 (2000.18), [M + K] ⁺ : 2016.17 (2016.16)	98.7%	18.9–21.0	−0.48 ± 0.14	144	> 100	IC ₅₀ : 1.26 ± 0.2 ^{[f][19]}
4/[⁶⁸ Ga]4 MALDI-MS (<i>m/z</i>) for [M + H] ⁺ (calcd): 1467.57 (1467.72), [M + Na] ⁺ : 1489.56 (1489.70), [M + K] ⁺ : 1505.90 (1505.68)	–	–	–	–	–	K _i : 47 ± 11 ^{[f][20]}
5/[⁶⁸ Ga]5 HR-ESI-MS (<i>m/z</i>) for [M + 6H] ⁶⁺ (calcd): 473.5914 (473.5921), [M + 5H] ⁵⁺ (calcd): 568.1081 (568.1089); MALDI-MS (<i>m/z</i>) for [M + H] ⁺ (calcd): 2836.28 (2836.51), [M + Na] ⁺ : 2858.78 (2858.50), [M + K] ⁺ : 2874.72 (2874.47)	96.0%	18.7–21.4	−2.47 ± 0.18	67	6	IC ₅₀ : 13 ± 3 ^{[e][17]}

[a] Radiochemical yield. [b] Non-optimized molar activity. [c] In human serum. [d] In human liver microsomal assay. [e] NPY(Y₁)R affinity of DOTA-modified peptide derivative. [f] NPY(Y₁)R affinity of native peptide derivative.

Chemical synthesis of chelator-modified peptides 1–5

Peptides 1–3 could be synthesized by applying standard Fmoc-based solid phase peptide synthesis (SPPS) protocols, standard Fmoc- N_α -amino acids, Fmoc-*L*-Bip-OH and Fmoc-*L*-Lys(lauroyl)-OH and HBTU (2-(1*H*-Benzotriazole-1-yl)-1,1,3,3-tetramethyluronium hexafluorophosphate) as coupling agent. To enable DOTA conjugation to the N_ϵ amino function of lysine, Fmoc-*L*-Lys(Mtt)-OH was used during the synthesis of the linear peptide sequences. After mild acidic cleavage of the Mtt protecting group with 1.5% TFA (trifluoroacetic acid) in CH_2Cl_2 , DOTA-tris(*t*Bu)ester was coupled using standard reaction conditions but PyBOP (benzotriazole-1-yl-oxy-tris-pyrrolidino-phosphonium hexafluoro-phosphate) activation and prolonged coupling times of 1 h.

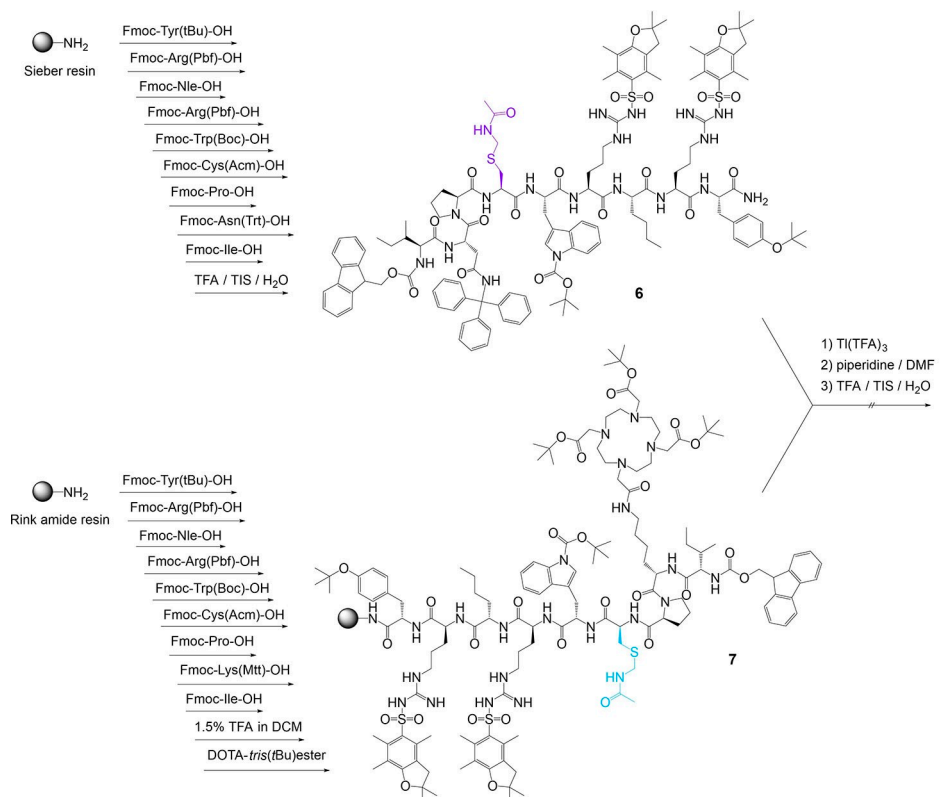
Compound 4 was synthesized accordingly, using the Ac-protected cysteine derivatives Fmoc-*D*-Cys(Acm)-OH and Fmoc-*L*-Cys(Acm)-OH during peptide assembly, followed by acetylation of the N-terminus by using acetic anhydride and DIPEA (*N,N*-diisopropylethylamine) in DMF. Afterwards, the oxidative deprotection and simultaneous cyclization of the peptide was carried out using $\text{Ti}(\text{TFA})_3$.

To obtain 5, a new synthetic strategy had to be established as the procedure described previously gave the product in insufficient yields of ~1% and low purity of only 83%.^[17] In the published protocol, both peptide monomers were synthesized according to a Boc-strategy and purified, then the *S*-Ac-protecting groups were removed by using silver trifluoro-

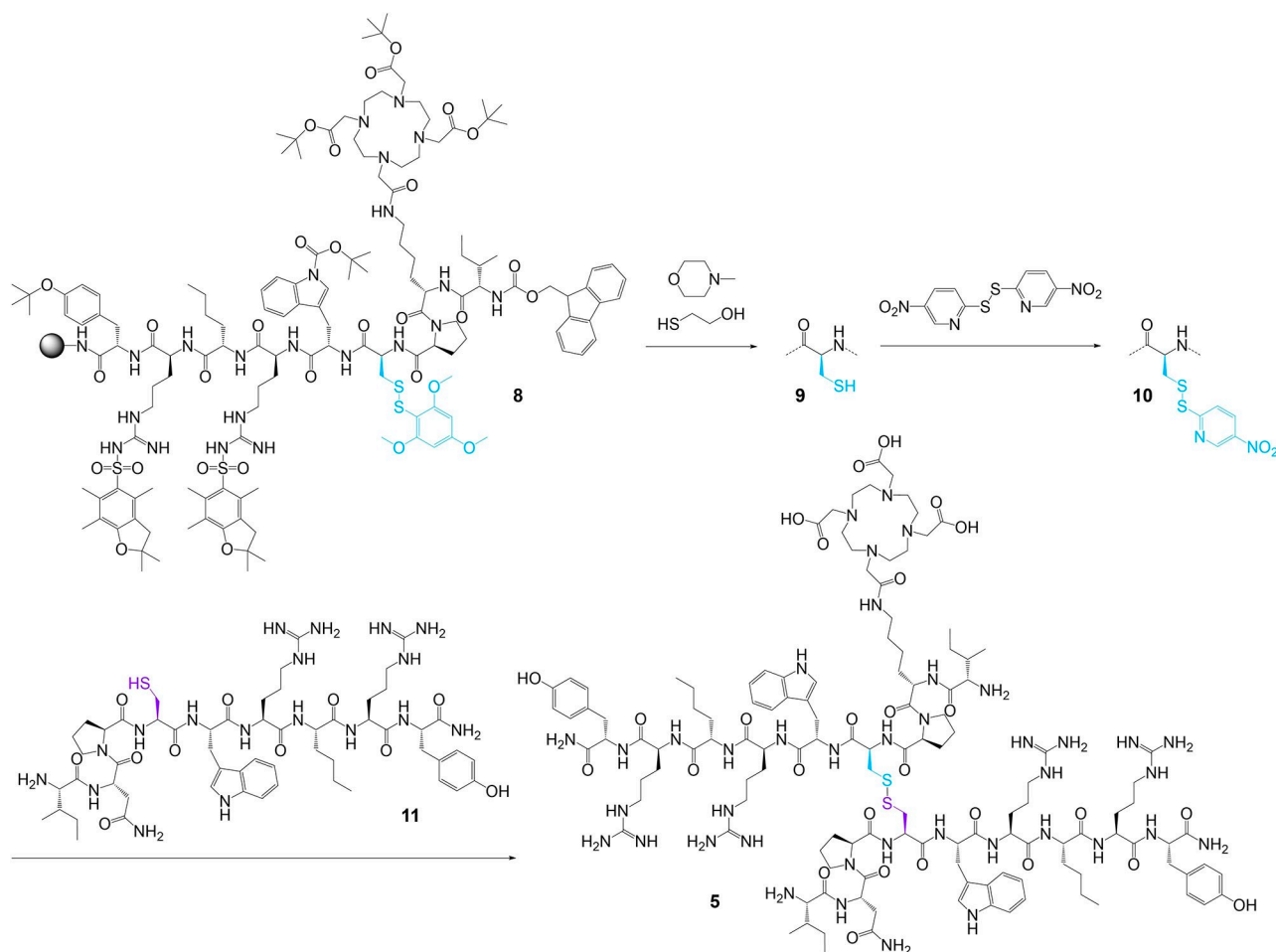
methane sulfonate. The heterodimer was subsequently obtained by reacting both monomers in equimolar amounts under oxidative conditions in solution, forming the intramolecular S–S-bond. Under these conditions, the main contaminants were the homodimers which could not be fully separated, resulting in the low product purity of 83%. In a first attempt to obtain 5 in pure form, we synthesized both peptide monomers 6 and 7 using standard Fmoc-based SPPS protocols and Fmoc-Cys(Acm)-OH as cysteine derivative during peptide synthesis (Scheme 1).

The non-DOTA-modified monomer was built on a highly acid-labile Sieber amide resin, giving the fully protected peptide 6 after mild acidic cleavage whereas the other, DOTA-modified monomer 7 was synthesized on a standard rink amide resin. Fully protected monomer 6 was then added in solution to the DOTA-modified peptide 7 (still on resin) together with $\text{Ti}(\text{TFA})_3$ to produce the peptide heterodimer on resin. After cleavage, only the intended heterodimer was expected to have formed. Unfortunately, this approach did not give the product 5 in sufficient yield as the formation of the dithiol bond showed to take place only to a very low extent, potentially due to the steric hindrance caused by the fully protected peptides.

Thus, another attempt was made using a different strategy, depicted in Scheme 2. First, we synthesized the deprotected asparagine-containing monomer 11 by standard Fmoc-based SPPS protocols. The DOTA-modified counterpart 8 was also obtained applying standard methods as described before, using Fmoc-Cys(STmp)-OH instead of standard Fmoc-Cys(Trt)-OH



Scheme 1. Depiction of the synthetic route towards 5 used initially. It did not give the product in sufficient yield and purity.



Scheme 2. Depiction of the improved synthesis pathway that yielded **5** in pure form.

during the synthesis of the linear peptide. The STmp-protecting group could be quantitatively removed under mild reductive conditions using 2-mercaptoethanol and *N*-methylmorpholine (NMM) in DMF within 15 minutes, yielding the free thiol intermediate **9** on solid support. This thiol could be modified with 2,2'-dithio-*bis*(5-nitropyridine) (DTNP), giving the heterodisulfide intermediate **10** which easily reacted chemoselectively with the thiol moiety in peptide **11**, forming peptide heterodimer **5** and giving the pure product in at least moderate yield of 8% after HPLC purification.

⁶⁸Ga-Radiolabeling and determination of the log_D of the peptide monomers [⁶⁸Ga]**1**–[⁶⁸Ga]**4** and heterodimer [⁶⁸Ga]**5**

The peptide monomers **1**–**4** and the heterodimer **5** were radiolabeled with ⁶⁸Ga³⁺ (obtained by fractionated elution of an IGG ⁶⁸Ge/⁶⁸Ga generator system) in aqueous acetate-buffered solution. The radiolabeling reaction itself took place at 99 °C within reaction times of 10 minutes at pH 3.5–4.0. The ⁶⁸Ga-labeled products [⁶⁸Ga]**1**–[⁶⁸Ga]**3** and [⁶⁸Ga]**5** could be obtained in high radiochemical yields and purities of 96–99% as well as

non-optimized molar activities of 18.8–23.1 GBq/μmol, starting from 376.6–461.0 MBq of ⁶⁸Ga³⁺.

In contrast, pure [⁶⁸Ga]**4** could not be obtained under these standard conditions, as the formation of a significant number of side products occurred which increased over time. We first assumed that this side product formation could be a result of thermal degradation or radiolysis during radiolabeling. However, thermal degradation could be ruled out to be the reason for the observed fragmentation as the precursor showed to be stable at elevated temperature of 99 °C. Additionally, the peak pattern during radiolabeling did not change when the reaction was conducted at lower temperature of 45 °C (apart from the increased fraction of free ⁶⁸Ga³⁺ in the radiolabeling reaction solution at this temperature). Neither did the presence of a high excess of ascorbic acid (10 mg) result in considerably higher product homogeneity, thus also excluding radiolysis as the reason for the observed formation of side product. In order to rule out any involvement of the thiols of the intramolecular dithiol bond in side-product formation, we added the reductive agent TCEP (*tris*(2-carboxyethyl)phosphine) to the reaction mixture. This did not result in a homogeneously radiolabeled product either. Furthermore, as the formation of side products was only observed for the radiolabeled agent, but not the

precursor (as is evident from the radio-HPLC and corresponding UV-HPLC traces), the origin of the observed side products remains inconclusive. Therefore, we omitted further characterization and stability testing of [⁶⁸Ga]4 due to its limited radiochemical stability.

In the following, the log_D values of the radiolabeled peptide monomers [⁶⁸Ga]1–[⁶⁸Ga]3 and the heterodimer [⁶⁸Ga]5 were determined as the log_D can significantly impact the *in vivo* clearance pathway of the respective compound (renal vs. hepatobiliary clearance).^[31,32] The log_D values were determined from the distribution coefficient of the respective radiotracer between phosphate buffer at pH 7.4 and octan-1-ol and are given in Table 1. As expected, the log_D values varied significantly, increasing from the highly hydrophilic [⁶⁸Ga]1 (log_D of -3.61 ± 0.37) to lipophilic [⁶⁸Ga]3 (log_D of -0.48 ± 0.14) due to the modification of the peptide with the lipophilic Bip amino acid and the lauroyl residue. [⁶⁸Ga]5 also showed a rather hydrophilic character (log_D of -2.47 ± 0.18).

Determination of the stability of peptide monomers [⁶⁸Ga]1–[⁶⁸Ga]3 and heterodimer [⁶⁸Ga]5 in human serum and human microsomal stability assay

As NPY was shown before to be mainly metabolized by proteolytic degradation in tissues associated with the nervous system as well as in serum,^[11] the stability of the radioligands [⁶⁸Ga]1–[⁶⁸Ga]3 and [⁶⁸Ga]5 was first to be determined by a human serum stability assay. This assay provides a good measure for radiotracer stability during blood pool circulation. Additionally, the stability of the compounds against degradation by liver enzymes was determined by an assay with human liver microsomes as metabolic degradation of some of the radioligands can be caused by liver enzymes as well. Especially [⁶⁸Ga]3 is supposed to show a considerable *in vivo* uptake in the liver due to its high lipophilicity. The human liver microsomal stability assay allows the assessment of the intrinsic metabolic clearance of substances by the human hepatobiliary cytochrome P450 system including degradation by cytochrome P450, oxidoreductase, cytochrome b₅, CYP1A2, CYP2A6, CYP2B6, CYP2C8, CYP2C9, CYP2C19, CYP2D6, CYP2E1, CYP3A4, CYP4A, and FMO.

In the stability assay performed in human serum, the radiotracers showed the formation of different, mostly hydrophilic metabolites and significant differences regarding the rate of degradation by peptidases, resulting in strongly differing serum half-lives of the compounds (Figure 2, Table 1).

⁶⁸Ga-[Lys⁴(DOTA)]-BVD15 ([⁶⁸Ga]1) showed – as expected from literature data^[12] – a low stability in human serum with a half-life of only 20 minutes. The replacement of the Tyr³² amino acid by artificial Bip in [⁶⁸Ga]2 however resulted in a considerable stabilization against degradation and substantially prolonged serum half-life to 65 minutes. The additional N-terminal lauroylation in [⁶⁸Ga]3 further improved the serum stability of the radiopeptide significantly, demonstrating a half-life of 144 minutes. This radiopeptide half-life is absolutely sufficient for ⁶⁸Ga-PET imaging purposes as PET scans using this

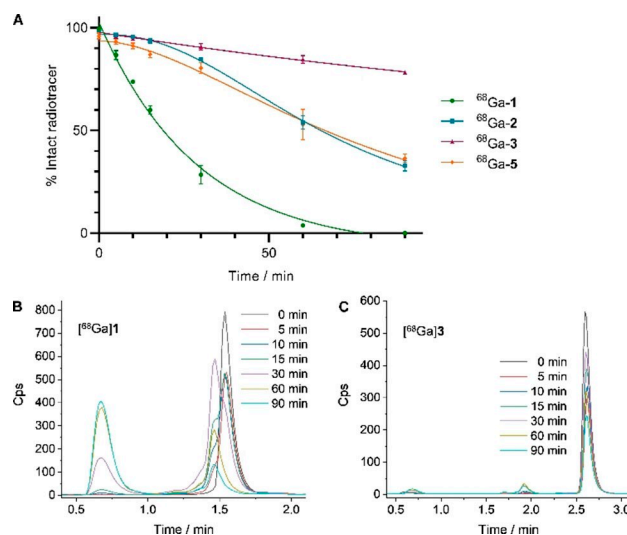


Figure 2. A) Results of the determination of the stability of [⁶⁸Ga]1–[⁶⁸Ga]3 and [⁶⁸Ga]5 in human serum and relevant parts of analytical radio-HPLC traces of exemplary serum stability experiments of B) [⁶⁸Ga]1 and C) [⁶⁸Ga]3. Error bars represent SD, all experiments were performed three times.

nuclide are usually performed within the first 60 to 90 minutes post injection. The heterodimer [⁶⁸Ga]5 demonstrated a serum half-life of 67 minutes, being comparable to that of [⁶⁸Ga]2.

As extensively studied before, NPY undergoes a proteolytic degradation mediated by a plethora of different peptidases, being present in the central and peripheral nervous system, cerebrospinal fluids and serum.^[9] In serum, the mainly active peptidase for NPY degradation was shown to be dipeptidyl peptidase 4 (DP4), N-terminally cleaving the peptide to exclusively give NPY₃₋₃₆ as the metabolite. Thus, DP4 cannot be the peptidase producing the degradation pattern observed in this study as the truncated peptides studied here lack the respective part of the NPY peptide being cleaved by this peptidase. Apart from DP4, also C-terminal angiotensin-converting enzyme (ACE)-mediated degradation was shown to take place in serum, giving metabolite NPY_{1-34r}, being thus more relevant for the observed enzymatic degradation of the truncated NPY analogues studied here. Further proteins which could be involved in the metabolization observed here are cathepsins, plasma Kallikrein and plasmin.^[9] The known cleavage pattern of truncated NPY₂₈₋₃₆ by these peptidases is depicted in Figure 3.

In the liver microsomal stability assay (using liver microsomes pooled from healthy human donors), a different radio-peptide degradation pattern was observed which was expected as a metabolization by liver enzymes involves completely different peptidases than those being present in serum. Consequently, other degradation half-lives were found for the studied radiopeptides (Figure 4, Table 1). In the line of [⁶⁸Ga]1 to [⁶⁸Ga]3, exhibiting an increasing number of artificial building blocks within the NPY sequence, the same stability trend was found as in the serum stability assay: [⁶⁸Ga]3, comprising an artificial Bip amino acid in position 32 as well as an N-terminal lauroyl modification showed the highest stability whereas the

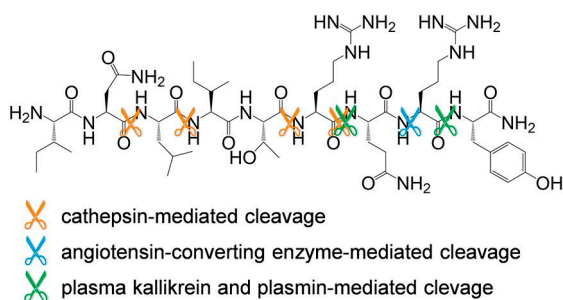


Figure 3. Known cleavage pattern of NPY₂₈₋₃₆ by different peptidases^[11]

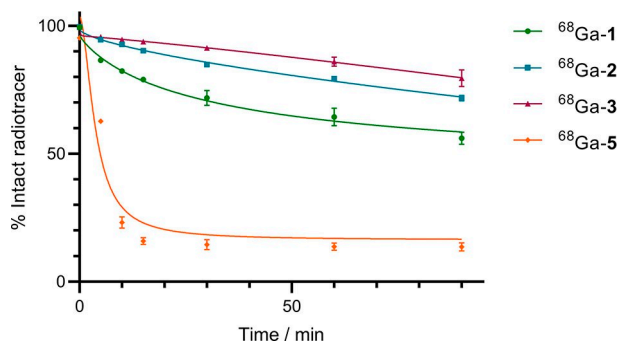


Figure 4. Results of the determination of the stability of [⁶⁸Ga]1–[⁶⁸Ga]3 and [⁶⁸Ga]5 in the human liver microsomal stability assay. Error bars represent SD, all experiments were performed three times.

modification with Bip alone resulted in a lower stability. The lowest stability in this row was again found for [⁶⁸Ga]1. In contrast to this, [⁶⁸Ga]5 was degraded much faster in the microsomal stability assay than in human serum. While it demonstrated a reasonable serum half-life of 67 minutes, it showed a very fast degradation by liver enzymes with a half-life of only 6 minutes. This is not *per se* astonishing as it has been shown before that *in vitro* stability assays performed in serum and tissue homogenates can yield different results.^[27] However, this behavior might also be attributable to the heterodimerization of the peptide, resulting in a structure strongly differing from that of the NPY lead, hampering the typical serum peptidase degradation by steric hindrance. In contrast, the structure of the peptide could provoke its metabolization by liver enzymes (e.g., by dithiol bridge cleavage and thiol oxidation or glutathione conjugation).

Taking the results of the serum stability and the liver microsomal stability assays together, [⁶⁸Ga]3 possesses the highest resistance against proteolytic degradation towards human serum as well as human liver peptidases. A further comparative testing of the agents in mice does not seem to be reasonable due to the different proteolytic activities towards peptides of human origin in both species,^[33] not allowing inferences on the stability of the agents in humans by studying it in rodents. Although these findings do not allow to predict a high *in vivo* stability of [⁶⁸Ga]3, thus potentially requiring further stabilization of the peptide sequence, the presented results are a good indication of the relative stabilities of the tested agents.

Taking furthermore into account that the peptide shows an excellent NPY(Y₁)R affinity profile, it demonstrates to be the most promising lead structure for the development of NPY(Y₁)R-specific imaging agents.

Conclusion

The most promising truncated NPY derivatives developed so far have been synthesized, in part modified for radiolabeling, radiolabeled with ⁶⁸Ga and in the following assessed towards their stability in human serum and human microsomal stability tests. This approach of testing in both systems is not only favorable, as it covers the main physiological degradation pathways for this NPY-based peptide class, but was also shown to be important, as both methods gave in part differing and complementary results. Thus, a much more precise prediction of the *in vivo* stability of the tested substances is possible combining both methods compared to serum stability testing alone.

Among the studied highly promising truncated NPY analogues, [Lys(lauroyl)²⁷,Pro³⁰,Lys(DOTA)³¹,Bip³²,Leu³⁴]NPY₂₇₋₃₆ ([⁶⁸Ga]3) not only shows excellent *in vitro* receptor binding properties (NPY(Y₁)R affinity and receptor agonism), but – in contrast to the other agents investigated – also a very high stability towards proteolytic degradation by peptidases in human serum and the human liver. It therefore represents the most promising lead compound for the further development of NPY(Y₁)R-specific molecular imaging agents.

Experimental Section

General. All commercially available chemicals were of analytical grade and were used without further purification. Resins for solid phase-based peptide syntheses, PyBOP and Fmoc-protected standard amino acids were purchased from NovaBiochem. Fmoc-L-Bip-OH and Fmoc-L-Lys(lauroyl)-OH were obtained from Iris Biotech. HBTU was purchased from Carl Roth and DOTA-tris(tBu)ester was obtained from CheMatech. Human serum and liver microsomes were obtained from Sigma-Aldrich.

For HPLC chromatography, a Dionex UltiMate 3000 system was used together with Chromeleon Software (Version 6.80). For analytical and semipreparative chromatography, Chromolith Performance (RP-18e, 100–4.6 mm, Merck, Germany) and Chromolith Semiprep (RP-18e, 100–10 mm, Merck, Germany) columns were used, respectively. For radioanalytical use, a Dionex UltiMate 3000 system equipped with a Raytest GABI Star radioactivity detector was used together with a Chromolith Performance (RP-18e, 100–4.6 mm, Merck, Germany) column. All operations were performed using H₂O + 0.1% TFA and MeCN + 0.1% TFA as solvents at a flow rate of 4 mL/min. HR-ESI (high-resolution electrospray ionization) and MALDI (matrix-assisted laser desorption/ionization) spectra were obtained with Finnigan MAT95Q and Bruker Daltronics Microflex spectrometers, respectively. Gamma counting was performed by using a 2480 Wizard gamma counter system from Perkin Elmer.

General synthesis of peptides (1–5). The peptides were synthesized on solid support by standard Fmoc solid-phase peptide synthesis protocols^[26,27] using standard commercially available

resins (Rink Amide MBHA resin, NovaSyn TG Sieber resin), HBTU as coupling agent and N_α -amino acids. The coupling reactions were carried out in DMF for 30 min using 4 equiv. of amino acid, 3.9 equiv. of HBTU as coupling reagent and 4 equiv. of DIPEA as base. For conjugation of DOTA-tris(tBu)ester, only 2 equiv. of acid were used, being activated with PyBOP instead of HBTU and the coupling time was prolonged to 1 h. Fmoc protecting groups were removed using 50% (v/v) piperidine in DMF within 7 min. Peptide cyclization by S–S-bond formation during the synthesis of **4** was carried out on resin applying the respective D- and L-Fmoc-Cys(Acm)-OH amino acids during peptide synthesis and 4 equiv. of $\text{Ti}(\text{TFA})_3$ in DMF (5 mL) for 45 min at ambient temperature. N-terminal acetylation of **4** was carried out using a mixture of acetic anhydride (50 equiv) and DIPEA (50 equiv) in DMF (1.5 mL) for 30 min at ambient temperature. **5** was obtained modifying a synthesis protocol for heterodisulfide-based heterodimeric peptides using DTNP.^[28] At first, the asparagine-containing peptide monomer was assembled using standard Fmoc-based SPPS methods. Analogously, the DOTA-modified peptide monomer was synthesized on solid support using Fmoc-Cys(STmp)-OH during peptide synthesis. The STmp-protecting group was removed on solid support, leaving all other protecting groups unaffected, by incubation of the resin with a solution of 2-mercaptoethanol (5%, v/v) in *N*-methylmorpholine in DMF (0.1 M, 5 mL) for 5 minutes. This step was repeated twice. After thorough washing of the resin with DMF, it was incubated with a solution of DTNP (5 equiv) in DMF (1 mL) for 1 h. After this time, the solution was replaced by fresh DTNP solution of the same composition and the reaction conducted for further 2 h. The resin was again washed thoroughly with DMF and incubated with a solution of asparagine-containing peptide monomer (1.25 equiv) in DMF (1 mL) overnight. The crude products were cleaved from the solid support using a mixture of TFA:TIS (triisopropylsilane) : H_2O (95:2.5:2.5 v/v/v) for 60 min, suspended in diethyl ether and purified by semipreparative HPLC. The products were isolated as white solids after lyophilization. Gradients used for HPLC purification and corresponding retention times, synthesis yields, and characterization data for each substance are given below.

Compound 1: gradient: 5–35% MeCN + 0.1% TFA in 6 min (t_{R} = 4.6 min), yield: 36% (86.9 mg), MALDI-MS (m/z) for $[M+H]^+$ (calcd): 1607.40 (1607.90), $[M+Na]^+$ (calcd): 1629.51 (1629.88), $[M+K]^+$ (calcd): 1645.50 (1645.86). HR-ESI-MS (m/z) for $[M+4H]^4+$ (calcd): 402.7305 (402.7314), $[M+3H]^3+$ (calcd): 536.6383 (536.6393), $[M+2H]^2+$ (calcd): 804.4537 (804.4550).

Compound 2: gradient: 20–40% MeCN + 0.1% TFA in 5 min (t_{R} = 3.6 min), yield: 31% (77.2 mg), MALDI-MS (m/z) for $[M+H]^+$ (calcd): 1667.83 (1667.94), $[M+Na]^+$ (calcd): 1689.90 (1689.92), $[M+K]^+$ (calcd): 1705.29 (1705.89). HR-ESI-MS (m/z) for $[M+4H]^4+$ (calcd): 417.7397 (417.7405), $[M+3H]^3+$ (calcd): 556.6504 (556.6514).

Compound 3: gradient: 35–42% MeCN + 0.1% TFA in 5 min (t_{R} = 4.2 min), yield: 30% (82.7 mg), MALDI-MS (m/z) for $[M+H]^+$ (calcd): 1978.01 (1978.20), $[M+Na]^+$ (calcd): 1999.95 (2000.18), $[M+K]^+$ (calcd): 2016.17 (2016.16). HR-ESI-MS (m/z) for $[M+4H]^4+$ (calcd): 495.2564 (495.3060), $[M+3H]^3+$ (calcd): 660.0712 (660.0721).

4: gradient: 20–25% MeCN + 0.1% TFA in 5 min (t_{R} = 2.4 min), yield: 28% (60.0 mg), MALDI-MS (m/z) for $[M+H]^+$ (calcd): 1467.57 (1467.72), $[M+Na]^+$ (calcd): 1489.56 (1489.70), $[M+K]^+$ (calcd): 1505.90 (1505.68).

5: gradient: 10–40% MeCN + 0.1% TFA in 8 min (t_{R} = 5.5 min), yield: 8% (32.0 mg), MALDI-MS (m/z) for $[M+H]^+$ (calcd): 2836.28 (2836.51), $[M+Na]^+$ (calcd): 2858.78 (2858.50), $[M+K]^+$ (calcd):

2874.72 (2874.47). HR-ESI-MS (m/z) for $[M+6H]^6+$ (calcd): 473.5914 (473.5921), $[M+5H]^5+$ (calcd): 568.1081 (568.1089).

^{68}Ga -radiolabeling of DOTA-modified peptides 1–5. A solution of the respective monomers or heterodimer (20 nmol) in Tracepur water (20 μL) was added to 376.6–461.0 MBq of $^{68}\text{Ga}^{3+}$ in a solution obtained by fractionated elution of a $^{68}\text{Ge}/^{68}\text{Ga}$ generator (IGG100, Eckert and Ziegler, Berlin, Germany) with HCl (0.1 M, 1.4–1.6 mL) and subsequent titration to pH 3.5–4.0 by addition of sodium acetate solution (1.25 M, 120–140 μL). After reaction for 10 min at 99 °C, the reaction mixtures were analyzed by analytical radio-HPLC. The radiolabeled products $[^{68}\text{Ga}]1$ – $[^{68}\text{Ga}]3$ and $[^{68}\text{Ga}]5$ were found to be 95–99% pure and obtained in non-optimized molar activities of 18.8–23.1 GBq/ μmol .

Determination of the \log_D of $[^{68}\text{Ga}]1$ – $[^{68}\text{Ga}]3$ and $[^{68}\text{Ga}]5$. The peptide monomers and heterodimer were radiolabeled with ^{68}Ga as described before and the pH of the product solutions was adjusted to 7.4 using HEPES buffer (2 M, pH 8, ~350 μL ; HEPES: 4-(2-hydroxyethyl)piperazine-1-ethanesulfonic acid). 2 μL of the product solution (~25 pmol of the respective ligand) were added to a mixture of phosphate buffer (0.05 M, pH 7.4, 800 μL) and octan-1-ol (800 μL) and incubated for 5 min at ambient temperature with vigorous shaking. Both phases were separated by centrifugation, and 100 μL of each phase were measured for radioactivity in a gamma-counter. From these data, the distribution coefficient \log_D was calculated from the following equation: $\log_{D_{o/w}} = \log(\text{cpm}_o / \text{cpm}_w)$, where: cpm_o = activity in the octan-1-ol phase (cpm = counts per minute) and cpm_w = activity in the aqueous phase. These experiments were performed thrice for each radioligand, each experiment in triplicate.

Determination of the stability of $[^{68}\text{Ga}]1$ – $[^{68}\text{Ga}]3$ and $[^{68}\text{Ga}]5$ in human serum. The peptide monomers and heterodimer were radiolabeled with ^{68}Ga as described before and 62.5 μL of the product solution were added to 250 μL of human serum and incubated at 37 °C. At defined time-points of 5, 10, 15, 30, 60 and 90 min, aliquots of 45 μL of the mixtures of $[^{68}\text{Ga}]1$ – $[^{68}\text{Ga}]3$ were added to 45 μL of ethanol and the precipitation of serum proteins was enhanced by ice-cooling for 2 min. The adhesion to serum proteins was determined to be between 3 and 7%. After centrifugation, the supernatant was analyzed by analytical radio-HPLC. For $[^{68}\text{Ga}]5$, showing a considerable adhesion to serum proteins of ~30%, the precipitation of serum proteins was omitted and the radiotracer-serum mixtures were directly analyzed by analytical radio-HPLC. These experiments were performed thrice for each ^{68}Ga -labeled compound.

Determination of the stability of $[^{68}\text{Ga}]1$ – $[^{68}\text{Ga}]3$ and $[^{68}\text{Ga}]5$ by microsomal stability assay.^[29] The peptide monomers and heterodimer were radiolabeled with ^{68}Ga as described before and the solution of the radiolabeled product was brought to pH 7.4 by addition of HEPES buffer (2 M, ~200 μL). 500 μL of this solution were added to 500 μL of a solution containing 2.6 mM NADP, 6.6 mM glucose 6-phosphate, 0.8 U/mL glucose 6-phosphate dehydrogenase and 6.6 mM MgCl_2 in 0.5 M potassium phosphate buffer, pH 7.4. To this mixture was added 1 mg/mL protein to initiate the reaction. At defined time-points of 5, 10, 15, 30, 60 and 120 min, aliquots of 100 μL of the mixture were added to 100 μL of acetonitrile and the precipitation of proteins was enhanced by ice-cooling for 2 min. After centrifugation, the supernatant was analyzed by analytical radio-HPLC. These experiments were performed thrice for each ^{68}Ga -labeled compound.

Acknowledgements

The authors gratefully acknowledge financial support from the German Research Foundation (grant number WA3555/1-1). Open access funding enabled and organized by Projekt DEAL.

Conflict of Interest

The authors declare no conflict of interest.

Keywords: NPY(Y₁)R · peptides · radiochemistry · stability · truncated NPY peptides

- [1] S. Hofmann, K. Bellmann-Sickert, A. G. Beck-Sickinger, *Biol. Chem.* **2019**, *400*, 299–311.
- [2] C. Cabrele, A. G. Beck-Sickinger, *J. Pept. Sci.* **2000**, *6*, 97–122.
- [3] M. Korner, J. C. Reubi, *Peptides* **2007**, *28*, 419–425.
- [4] J. C. Reubi, M. Gugger, B. Waser, J. C. Schaer, *Cancer Res.* **2001**, *61*, 4636–4641.
- [5] J. C. Reubi, M. Gugger, B. Waser, *Eur. J. Nucl. Med. Mol. Imaging* **2002**, *29*, 855–862.
- [6] H. J. Wester, H. Kessler, *J. Nucl. Med.* **2005**, *46*, 1940–1945.
- [7] S. Hoffmann, B. Rist, G. Videnov, G. Jung, A. G. Beck-Sickinger, *Regul. Pept.* **1996**, *65*, 61–70.
- [8] Z. L. Yang, S. Han, M. Keller, A. Kaiser, B. J. Bender, M. Bosse, K. Burkert, L. M. Kogler, D. Wifling, G. Bernhardt, N. Plank, T. Littmann, P. Schmidt, C. Y. Yi, B. B. Li, S. Ye, R. G. Zhang, B. Xu, D. Larhammar, R. C. Stevens, D. Huster, J. Meiler, Q. Zhao, A. G. Beck-Sickinger, A. Buschauer, B. L. Wu, *Nature* **2018**, *556*, 520–524.
- [9] M. Werle, A. Bernkop-Schnurch, *Amino Acids* **2006**, *30*, 351–367.
- [10] C. Rangger, R. Haubner, *Pharmaceuticals* **2020**, *13*, 22.
- [11] L. Wagner, R. Wolf, U. Zeitschel, S. Rossner, A. Petersen, B. R. Leavitt, F. Kastner, M. Rothermundt, U. T. Gartner, D. Gundel, D. Schlenzig, N. Frerker, J. Schade, S. Manhart, J. U. Rahfeld, H. U. Demuth, S. von Horsten, *J. Neurochem.* **2015**, *135*, 1019–1037.
- [12] D. Zwanziger, I. Bohme, D. Lindner, A. G. Beck-Sickinger, *J. Pept. Sci.* **2009**, *15*, 856–866.
- [13] I. U. Khan, R. Reppich, A. G. Beck-Sickinger, *Biopolymers* **2007**, *88*, 182–189.
- [14] M. J. Liu, S. J. Mountford, L. Zhang, I. C. Lee, H. Herzog, P. E. Thompson, *Int. J. Pept. Res. Ther.* **2013**, *19*, 33–41.
- [15] C. Zhang, J. Pan, K. S. Lin, I. Dude, J. Lau, J. Zeisler, H. Merckens, S. Jenni, B. Guerin, F. Benard, *Mol. Pharmaceutics* **2016**, *13*, 3657–3664.
- [16] X. Li, D. Yang, *Chem. Commun.* **2006**, *32*, 3367–3379.
- [17] D. Chatenet, R. Cescato, B. Waser, J. Ercegyi, J. E. Rivier, J. C. Reubi, *EJNMMI Res.* **2011**, *1*, 21–31.
- [18] B. Guerin, V. Dumulon-Perreault, M. C. Tremblay, S. Ait-Mohand, P. Fournier, C. Dubuc, S. Authier, F. Benard, *Bioorg. Med. Chem. Lett.* **2010**, *20*, 950–953.
- [19] S. Hofmann, J. Lindner, A. G. Beck-Sickinger, E. Hey-Hawkins, K. Bellmann-Sickert, *ChemBioChem* **2018**, *19*, 2300–2306.
- [20] Y. Takebayashi, H. Koga, J. Togami, A. Inui, H. Kurihara, K. Koshiya, T. Furuya, A. Tanaka, K. Murase, *J. Pept. Res.* **2000**, *56*, 409–415.
- [21] N. Koglin, C. Zorn, R. Beumer, C. Cabrele, C. Bubert, N. Sewald, O. Reiser, A. G. Beck-Sickinger, *Angew. Chem. Int. Ed.* **2003**, *42*, 202–205.
- [22] M. Pourghasian, J. Inkster, N. Hundal, F. Mesak, B. Guerin, S. Ait-Mohand, T. Ruth, M. Adam, K. S. Lin, F. Benard, *J. Nucl. Med.* **2011**, *52*, S1685.
- [23] B. J. Evans, A. T. King, A. Katsifis, L. Matesic, J. F. Jamie, *Molecules* **2020**, *25*, 2314.
- [24] B. A. Nock, T. Maina, E. P. Krenning, M. de Jong, *J. Nucl. Med.* **2014**, *55*, 121–127.
- [25] A. Kaloudi, B. A. Nock, E. Lympers, R. Valkema, E. P. Krenning, M. de Jong, T. Maina, *EJNMMI Res.* **2016**, *6*, 15.
- [26] S. Richter, M. Wuest, C. N. Bergman, S. Krieger, B. E. Rogers, F. Wuest, *Mol. Pharmaceutics* **2016**, *13*, 1347–1357.
- [27] M. Ocak, A. Helbok, C. Rangger, P. K. Peitl, B. A. Nock, G. Morelli, A. Eek, J. K. Sosabowski, W. A. P. Breeman, J. C. Reubi, C. Decristoforo, *Eur. J. Nucl. Med. Mol. Imaging* **2011**, *38*, 1426–1435.
- [28] M. Klingler, C. Decristoforo, C. Rangger, D. Summer, J. Foster, J. K. Sosabowski, E. von Guggenberg, *Theranostics* **2018**, *8*, 2896–2908.
- [29] E. M. Parker, C. K. Babij, A. Balasubramaniam, R. E. Burrier, M. Guzzi, F. Hamud, G. Mukhopadhyay, M. S. Rudinski, Z. Tao, M. Tice, L. Xia, D. E. Mullins, B. G. Salisbury, *Eur. J. Pharmacol.* **1998**, *349*, 97–105.
- [30] M. E. Cardoso, E. Tejeria, A. M. Rey Rios, M. Teran, *Chem. Biol. Drug Des.* **2020**, *95*, 302–310.
- [31] S. Niedermoser, J. Chin, C. Wängler, A. Kostikov, V. Bernard-Gauthier, N. Vogler, J. P. Soucy, A. J. McEwan, R. Schirmacher, B. Wängler, *J. Nucl. Med.* **2015**, *56*, 1100–1105.
- [32] E. G. Garayoa, C. Schweinsberg, V. Maes, L. Brans, P. Blauenstein, D. A. Tourwe, R. Schibli, P. A. Schubiger, *Bioconjugate Chem.* **2008**, *19*, 2409–2416.
- [33] A. Ghosh, N. Raju, M. Tweedle, K. Kumar, *Cancer Biother. Radiopharm.* **2017**, *32*, 24–32.

Manuscript received: June 16, 2020
Revised manuscript received: July 17, 2020
Accepted manuscript online: July 17, 2020
Version of record online: August 7, 2020